Vacuum Beam Guide for Large Scale Quantum Networks

Yuexun Huang,[1,*] Francisco Salces–Carcoba,[2] Rana X. Adhikari,[2] Amir H. Safavi-Naeini,[3] and Liang Jiang[1,†]

[1]Pritzker School of Molecular Engineering, University of Chicago, Chicago, Illinois 60637, USA

[2]Division of Physics, Math, and Astronomy, LIGO Laboratory, California Institute of Technology, Pasadena, California 91125, USA

[3]Department of Applied Physics and Ginzton Laboratory, Stanford University, Stanford, California 94305, USA

(Received 21 December 2023; accepted 3 June 2024; published 9 July 2024)

The vacuum beam guide (VBG) presents a completely different solution for quantum channels to overcome the limitations of existing fiber and satellite technologies for long-distance quantum communication. With an array of aligned lenses spaced kilometers apart, the VBG offers ultrahigh transparency over a wide range of optical wavelengths. With realistic parameters, the VBG can outperform the best fiber by 3 orders of magnitude in terms of attenuation rate. Consequently, the VBG can enable long-range quantum communication over thousands of kilometers with quantum channel capacity beyond 10^{13} qubit/sec, orders of magnitude higher than the state-of-the-art quantum satellite communication rate. Remarkably, without relying on quantum repeaters, the VBG can provide a ground-based, low-loss, high-bandwidth quantum channel that enables novel distributed quantum information applications for computing, communication, and sensing.

DOI: 10.1103/PhysRevLett.133.020801

It is an outstanding challenge to build an effective low-loss quantum channel for global-scale quantum networks, which will enable transformative applications of secure quantum communication [1], distributed quantum sensing [2], and network-based quantum computation [3,4]. The main obstacle is the absorption loss of optical channels, with attenuation length limited to tens of kilometers for fiber and free-space channels, resulting in an exponential decrease in the direct quantum communication rate over long distances. Significant progress has been made in extending the communication distances for quantum networks, including satellite-based quantum entanglement distribution over 1200 km [5] and memory-enhanced quantum communication [6] beyond the repeater-less bounds [7,8]. However, satellite-based quantum channels are fragile, expensive, and restricted by local weather conditions [9,10]. Furthermore, quantum repeaters without full quantum error correction will still suffer from a polynomial decrease in communication rate over long distances [11]. Hence, it is highly desirable to establish a reliable quantum channel capable of directly transmitting quantum signals over vast distances, such as the continental scale of 10^4 km (with an attenuation rate of at the level of 10^{-4} dB/km) for a wide range of optical frequencies.

To overcome this challenge, we explore a completely different approach—the vacuum beam guide (VBG)—which uses an array of lenses (in an evacuated tube) to guide light, as opposed to relying on total reflection induced by fiber. The large vacuum spacing between lenses significantly reduces the effective travel length of light in optical materials, thus eliminating the problem of material absorption. Inspired by quantum communication satellites, the VBG channel is set up within a vacuum chamber tube, which eliminates air absorption and effectively isolates the channel from the outer environment, ensuring robustness against environmental perturbations. Although beam waveguides were proposed for classical optical communication [12], it was taken over by low-cost optical fiber, which is sufficient for classical communication, despite its intrinsic loss. For quantum communication, however, it is crucial that the design of the vacuum beam guide has the potential to achieve ultra-low-loss long-distance communication. With the ability to build large-scale vacuum chambers hosting precision optical elements separated by multiple kilometers, we can make exciting scientific discoveries, such as gravitational wave detection by the Laser Interferometer Gravitational-wave Observatory (LIGO) [13].

Here, we propose deploying the VBG as the backbone quantum channel toward a global quantum network with a hierarchy structure as shown in Figs. 1(a) and 1(b). We model the system and estimate the upper bound of the attenuation dominated by residue air absorption, optical losses introduced by lenses, and misalignment of the beam guide. Our estimation demonstrates the VBG as state-of-the-art under a practical and exemplifying configuration, establishing it as one of the most practical and potentially useful quantum communication techniques at a global scale.

Ultrahigh transmission of VBG.—The VBG is a long vacuum chamber tube that consists of an array of N_{tot} lenses spaced L_0 apart, which enables the connection of quantum terminals separated by $L_{\mathrm{tot}} = N_{\mathrm{tot}} L_0$, as illustrated in Fig. 1(c). The vacuum has a typical pressure below $\sim$1 Pa, which ensures low absorption from the remaining gas at room temperature. The lenses are shielded from seismic vibrations and are optically aligned with adaptive

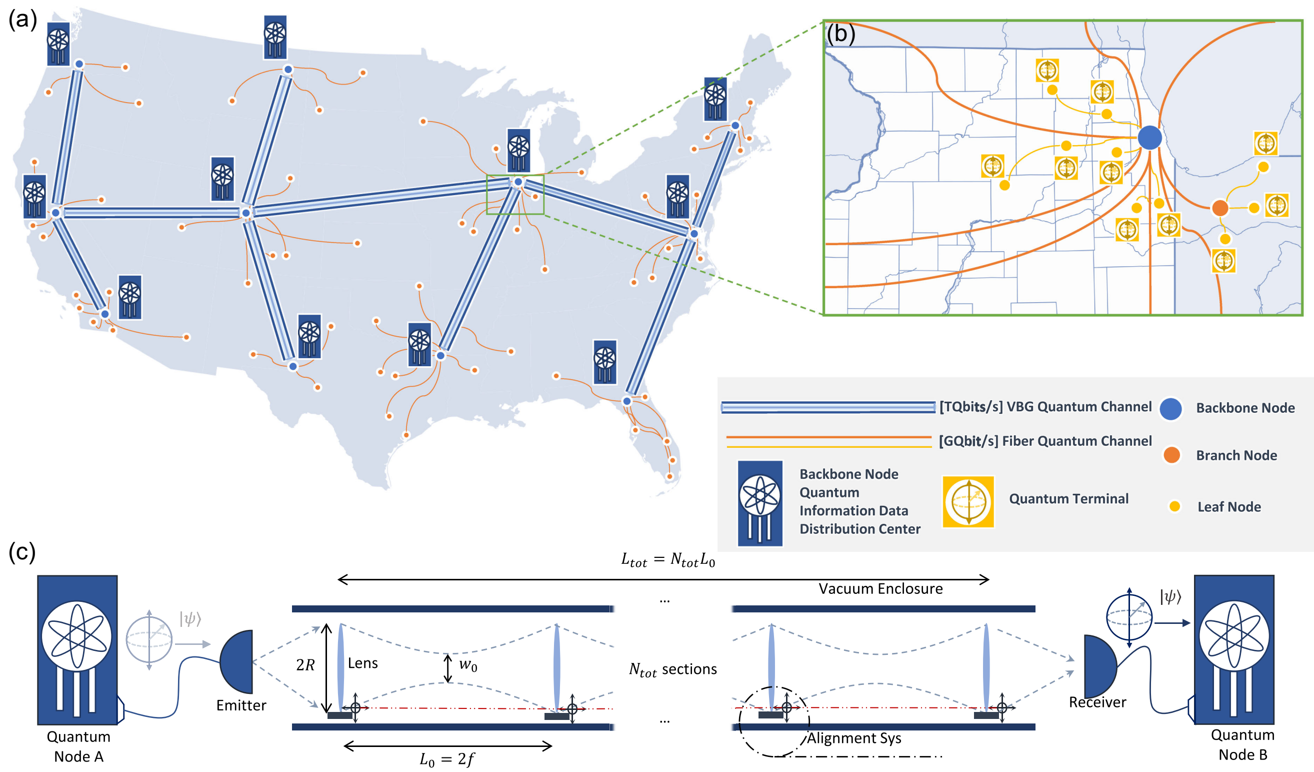

FIG. 1. A hierarchical structure of large-scale quantum networks connected by vacuum beam guides (VBGs). (a) The VBG backbone network (blue links) can transfer quantum information with high capacity (with TeraQubits/ sec) over long distances, connecting regional quantum networks (orange links). (b) The regional network consists of fiber or free-space quantum channels designed to distribute quantum information to branch nodes and quantum terminals (with GigaQubits/ sec) across urban scales. (c) The design of the VBG involves placing lenses with identical focus length f and radius R at regular intervals within a vacuum chamber tube, constructing a VBG with $N_{\rm tot}$ sections. The positions of the lenses are stabilized by an advanced alignment system. In the VBG, the fundamental Gaussian mode with waist w_0 can travel at an extremely low loss over a distance of $L_{\rm tot}$. Quantum states can be transferred from quantum node A at one end of the VBG to quantum node B at the other end of the VBG.

feedback. In this analysis, we consider a feasible and robust confocal design with a spacing of $L_0 = 4$ km and a focal length of $f = L_0/2$. The beam waist is $w_0 = \sqrt{\lambda f/\pi} \approx 3$ cm for the telecom-band wavelength λ. The lens radius of $R = 12$ cm is sufficient to achieve negligible diffraction loss.

Optical signals encoding quantum information can transmit through the VBG with little loss, even after passing through an array of aligned lenses over thousands of kilometers. The effective attenuation rate (in units of dB/km) characterizes the VBG transmission loss, with three major contributions associated with the lens, residual gas, and imperfect alignment:

$$\alpha_{\rm tot} = \alpha_{\rm lens} + \alpha_{\rm gas} + \alpha_{\rm align}. \tag{1}$$

We now discuss the conditions to achieve an attenuation rate at the level of 10^{-4} dB/km for all three contributions.

The lens loss, $\alpha_{\rm lens}$, is associated with absorption, scattering, reflection, and diffraction. As illustrated in Fig. 2(a), a lens radius of $R \geq 12$ cm is adequate to suppress diffraction loss for $L_0 = 4$ km. Furthermore, by adding a multilayer antireflective coating, the total loss per lens can be reduced to less than 10^{-4}, resulting in an effective loss rate of $\alpha_{\rm lens} < 10^{-4}$ dB/km at the wavelengths $\lambda \approx 1550$ nm, which can match the telecom band [14].

Optical loss from residual gas in the VBG is primarily due to absorption. As shown in Fig. 2(b), we compute the attenuation rate $\alpha_{\rm gas}$ at various levels of gas pressure with the absorption computed based on the HITRAN database [35]. At a pressure of 1 Pa, the attenuation rate is $\alpha_{\rm gas} < 10^{-4}$ dB/km for optical wavelengths within the selected telecom bands. Further reducing the air pressure below 10^{-2} Pa is sufficient to achieve negligible air absorption by reducing attenuation rate below 10^{-4} dB/km almost over the entire spectrum. Increasing the pressure much above 1 Pa will lead to increased acoustic coupling [36].

We can derive an upper bound for the effective attenuation rate induced by imperfect alignment in the confocal design:

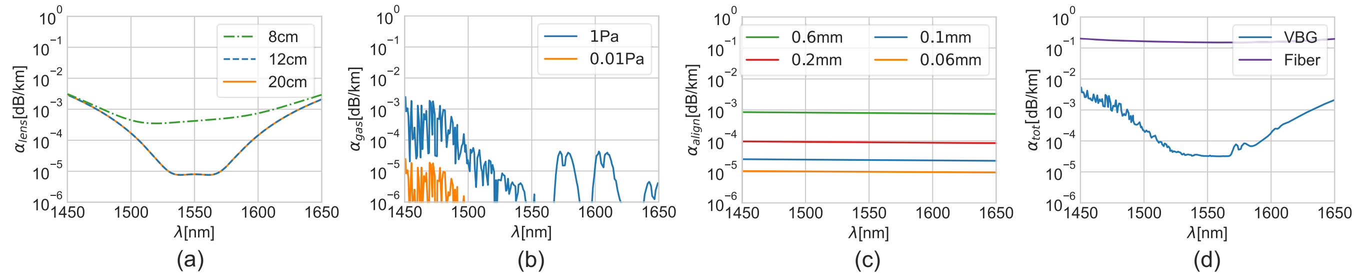

FIG. 2. Different effective attenuation rates as a function of wavelength under various configurations. (a) Attenuation rate from the lenses, $\alpha_{\rm lens}$, with lens radius $R = 8$, 12, 20 cm. For a large radius ($R \geq 12$ cm), the lens loss is limited by residual reflection and absorption from the AR coating. (b) Attenuation rate due to residual gas, $\alpha_{\rm gas}$, with moderate vacuum pressures: $P = 0.01$, 1 Pa. (c) The misalignment attenuation rate, $\alpha_{\rm align}$, with random transverse displacements $\sigma_s = 0.06$, 0.1, 0.2, 0.6 mm while fixing $(\sigma_{L_0}/L_0) = (\sigma_f/f) = 0.1\%$. (d) The total attenuation rate of the VBG compared to the advanced fiber [33,34] under the configuration of $L_0 = 4$ km, $R = 12$ cm, $P = 1$ Pa, and $\sigma_s = 0.1$ mm.

$$\alpha_{\rm align} \leq -\frac{10}{L_0}\log_{10}\left[1 - \frac{2\sigma_s^2}{w_0^2} - \frac{\sigma_{L_0}^2}{L_0^2} - \frac{\sigma_f^2}{f^2}\right], \qquad (2)$$

where σ_s and σ_{L_0} are the magnitudes of the fluctuations of transverse and longitudinal displacements for each lens, and σ_f is the deviation of the focal length. The general bound for $\alpha_{\rm align}$ for near confocal design is derived in Supplemental Material [14]. Since $w_0 \ll L_0, f$, the fluctuating transverse displacement is the dominant cause of attenuation, while the other two contributions can be sufficiently small, $(\sigma_{L_0}/L_0), (\sigma_f/f) < 10^{-3}$, achievable with current technology [14]. As illustrated in Fig. 2(c), it is essential to have good transverse alignment (e.g., $\sigma_s < 0.2$ mm) to achieve a low effective attenuation rate ($\alpha_{\rm align} < 10^{-4}$ dB/km). Even with relatively poor alignment (e.g., $\sigma_s = 0.6$ mm), we can still achieve $\alpha_{\rm align} < 10^{-3}$ dB/km, which is much better than the attenuation rate of fiber by at least an order of magnitude. Practically, each lens will be actively positioned using slow actuators, based on standard alignment sensing systems [37], bringing the residual miscentering to < 0.1 mm.

By summing up all three contributions, we can plot the total attenuation rate along with the individual contributions in Fig. 2(d), assuming practical parameters such as $R = 12$ cm, $P = 1$ Pa, and $\sigma_s = 0.1$ mm. The VBG can achieve an attenuation level as low as 3×10^{-5} dB/km for an optimized choice of wavelength within the atmospheric window, which corresponds to an effective attenuation length of 80 000 km, more than 3 orders of magnitude better than state-of-the-art fiber technology.

Quantum channel capacities of VBG.—We can use the VBG as a highly transparent bosonic quantum channel to transmit quantum information over long distances [38]. The VBG has a transmission efficiency at wavelength λ

$$\eta[\lambda] = 10^{-0.1 L_{\rm tot}\alpha[\lambda]}, \qquad (3)$$

which can be used for various quantum communication protocols. For one-way quantum communication (e.g., from Alice to Bob only), the one-way pure-loss capacity for a single wave packet at a wavelength λ is given by

$$q_1[\lambda] = \max\left[\log_2\left(\frac{\eta[\lambda]}{1-\eta[\lambda]}\right), 0\right], \qquad (4)$$

which vanishes for $\eta[\lambda] \leq 1/2$. If the pure-loss VBG channel is further assisted by two-way classical communication (between Alice and Bob), the corresponding two-way pure-loss capacity at a wavelength λ is [8]

$$q_2[\lambda] = \log_2\left(\frac{1}{1-\eta[\lambda]}\right), \qquad (5)$$

which is finite for all $\eta[\lambda] > 0$.

As shown in the insets of Fig. 3, the VBG can have a broad band with a large one-way or two-way channel capacity over long distances. In the low-loss regime with $L_{\rm tot} \ll 1/\alpha$, efficient multimode encoding techniques can be used to approach the asymptotic scaling of one-way channel capacity [39].

We can calculate the frequency-integrated channel capacity, which provides the maximum transmission rate of quantum information, by integrating over the frequency [40]:

$$Q_{1({\rm or}\,2)} \equiv \int q_{1({\rm or}\,2)} d\nu = \int q_{1({\rm or}\,2)}[\lambda]\frac{c}{\lambda^2}d\lambda, \qquad (6)$$

for one-way and two-way quantum communication protocols, respectively. The VBG has a significant advantage over other techniques, particularly due to its ultralow attenuation rate over a wide range of wavelengths, leading to an extremely large quantum capacity exceeding 10^{13} qubits/second over a distance of 10^4 km under one-way quantum communication protocol as shown in Fig. 3(a). While the estimation in Fig. 3(b) suggests that even with a baseline coupling loss as large as 50%, where the one-way

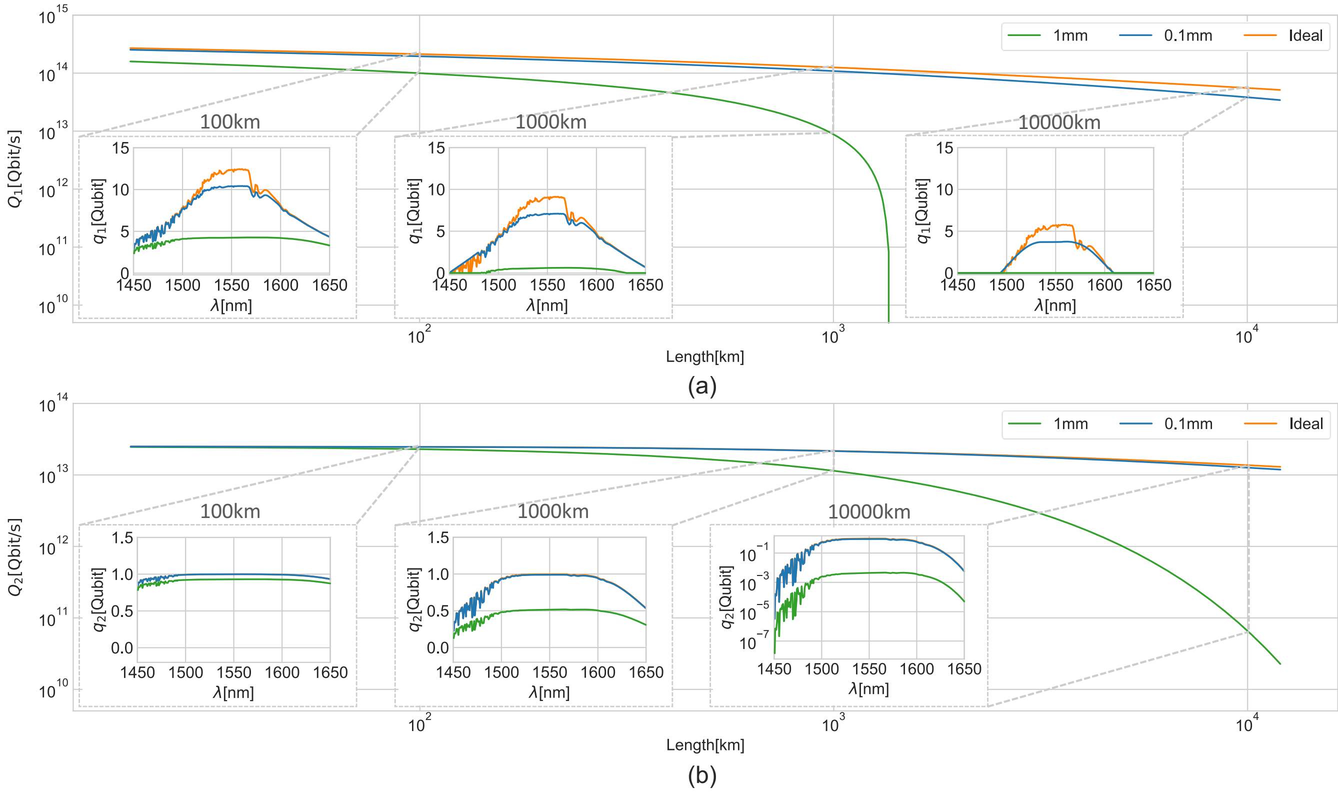

FIG. 3. The quantum channel capacity $Q_{1(or2)}$ at 1 Pascal as a function of transmission distance with $\sigma_s = 0.1$, 1 mm when fixing $(\sigma_{L_0}/L_0) = (\sigma_f/f) = 0.1\%$ compared to the ideal alignment. (a) One-way frequency-integrated quantum capacity with perfect coupling. (b) Two-way frequency-integrated quantum capacity assuming 50% coupling efficiency. The insets show the relation between channel capacity $q_{1(\mathrm{or}\,2)}$ as a function of wavelength at $L = 100$, 1000, 10 000 km. The inset of 10 000 km in (b) is in log scale to show finite two-way quantum capacity over a wide range of parameters.

protocol fails, it is still possible to achieve a Tera-level qubit rate via two-way protocols for continental scale communication. This points out a practically feasible pathway toward ultrafast global quantum networks.

While satellite techniques may offer advantages in mobility and coverage [41,42], the ground-based VBG offers high reliability as it is operational at all times, robust to environmental disturbance, and provides extremely high throughput, with achievable quantum communication rate at least 4 orders of magnitude higher [14]. The concept of a beam guide [12] was investigated to address diffraction loss in satellite-relayed quantum communication [10]. Nevertheless, that protocol remains susceptible to atmospheric and turbulence-induced losses, thereby affecting reliability, transmission rate, channel capacity, and communication latency (due to the limitation of two-way quantum communication). Additionally, unlike quantum repeaters [43], the VBG only requires passive optical lenses to focus the optical beams and does not need any quantum memory or active quantum devices to perform quantum error detection or correction. Therefore, the VBG should be feasible to implement with current technology.

Discussion.—We may also design the VBG to operate with visible light, which could take advantage of a broader air transmission window and low-loss lens materials. However, this approach demands stricter requirements in terms of lens surface roughness, beam alignment, and the mitigation of the UV absorption tail at visible wavelength.

The construction of VBG demands a considerable amount of investment and engineering effort. Additionally, maintaining the low pressure and the alignment of lenses in VBG also requires careful engineering. Nevertheless, we have already shown that such construction is feasible in principle, drawing from the vast experience gained from the development of LIGO. Pursuing this endeavor is undoubtedly worthwhile, given the unprecedented advantages it offers. In practice, there will be a trade-off between the VBG's performance and cost, and we can optimize its design parameters to achieve the desired balance.

Summary and outlook.—We have presented a ground-based VBG scheme that enables the implementation of a highly transparent and reliable optical quantum channel with an effective attenuation length of over 10^4 km and a large communication bandwidth. With currently available technology, the VBG can establish a continuous quantum channel connecting remote quantum devices with an ultrahigh quantum capacity above 10^{13} qubits/sec over continental scales, orders of magnitude higher than other approaches using satellites and quantum repeaters.

By addressing the challenge of lossy quantum channels, our high-throughput VBG has the potential to revolutionize quantum networks. The immediate and promising application of VBG will include various quantum key distribution schemes such as MDI-QKD [44,45], TF-QKD [46,47], and even DI-QKD [48–51]. The latter is particularly challenging for satellite-to-ground links due to the inevitable absorption loss of 3–8 dB [42] introduced by the thickness of the atmosphere. Furthermore, the VBG will enable a wide range of other exciting novel quantum network applications, including global-scale secure quantum communication [1], ultra-long-based optical telescopes [2], quantum network of clocks [52], quantum data centers [53], and delegated quantum computing [54,55].

We thank David Awschalom, Saikat Guha, Aaron Goodwin-Jones, Dan Brown, Ming Lai, John Preskill, and Peter Zoller for helpful comments and discussions. We acknowledge support from the ARO (No. W911NF-23-1-0077), ARO MURI (No. W911NF-21-1-0325), AFOSR MURI (No. FA9550-19-1-0399, No. FA9550-21-1-0209, No. FA9550-23-1-0338), NSF (No. PHY-0823459, No. PHY-1764464, No. ECCS-1941826, No. OMA-1936118, No. ERC-1941583, No. OMA-2137642, No. OSI-2326767, No. CCF-2312755), NTT Research, Packard Foundation (No. 2020-71479), and the Marshall and Arlene Bennett Family Research Program. This material is based upon work supported by the U.S. Department of Energy, Office of Science, National Quantum Information Science Research Centers.

[*]Contact author: yesunhuang@uchicago.edu
[†]Contact author: liang.jiang@uchicago.edu

[1] F. Xu, X. Ma, Q. Zhang, H.-K. Lo, and J.-W. Pan, Secure quantum key distribution with realistic devices, Rev. Mod. Phys. **92**, 025002 (2020).
[2] D. Gottesman, T. Jennewein, and S. Croke, Longer-baseline telescopes using quantum repeaters, Phys. Rev. Lett. **109**, 070503 (2012).
[3] H. J. Kimble, The quantum internet, Nature (London) **453**, 1023 (2008).
[4] S. Wehner, D. Elkouss, and R. Hanson, Quantum internet: A vision for the road ahead, Science **362**, eaam9288 (2018).
[5] J. Yin *et al.*, Satellite-based entanglement distribution over 1200 kilometers, Science **356**, 1140 (2017).
[6] M. K. Bhaskar, R. Riedinger, B. Machielse, D. S. Levonian, C. T. Nguyen, E. N. Knall, H. Park, D. Englund, M. Lončar, D. D. Sukachev, and M. D. Lukin, Experimental demonstration of memory-enhanced quantum communication, Nature (London) **580**, 60 (2020).
[7] M. Takeoka, S. Guha, and M. M. Wilde, Fundamental rate-loss tradeoff for optical quantum key distribution, Nat. Commun. **5**, 5235 (2014).
[8] S. Pirandola, R. Laurenza, C. Ottaviani, and L. Banchi, Fundamental limits of repeaterless quantum communications, Nat. Commun. **8**, 15043 (2017).
[9] S.-K. Liao *et al.*, Satellite-to-ground quantum key distribution, Nature (London) **549**, 43 (2017).
[10] S. Goswami and S. Dhara, Satellite-relayed global quantum communication without quantum memory, Phys. Rev. Appl. **20** (2023).
[11] S. Muralidharan, L. Li, J. Kim, N. Lütkenhaus, M. D. Lukin, and L. Jiang, Optimal architectures for long distance quantum communication, Sci. Rep. **6**, 20463 (2016).
[12] G. Goubau, Beam waveguides, Adv. Microwaves **3**, 67 (1968).
[13] B. P. Abbott *et al.*, Observation of gravitational waves from a binary black hole merger, Phys. Rev. Lett. **116**, 061102 (2016).
[14] See Supplemental Material at http://link.aps.org/supplemental/10.1103/PhysRevLett.133.020801 for the details of derivation, which includes Refs. [5,15–32].
[15] B. Abbott, R. Abbott, R. Adhikari, P. Ajith, B. Allen, G. Allen, R. Amin, S. Anderson, W. Anderson, M. Arain *et al.*, LIGO: The laser interferometer gravitational-wave observatory, Rep. Prog. Phys. **72**, 076901 (2009).
[16] J. C. Heurtley and W. Streifer, Optical resonator modes-circular reflectors of spherical curvature, J. Opt. Soc. Am. **55**, 1472 (1965).
[17] A. Yariv and P. Yeh, *Photonics: Optical Electronics in Modern Communications*, 6th ed., The Oxford Series in Electrical and Computer Engineering (Oxford University Press, New York, 2007).
[18] L. Pinard, C. Michel, B. Sassolas, L. Balzarini, J. Degallaix, V. Dolique, R. Flaminio, D. Forest, M. Granata, B. Lagrange *et al.*, Mirrors used in the LIGO interferometers for first detection of gravitational waves, Appl. Opt. **56**, C11 (2017).
[19] L. Pinard, B. Sassolas, R. Flaminio, D. Forest, A. Lacoudre, C. Michel, J. Montorio, and N. Morgado, Toward a new generation of low-loss mirrors for the advanced gravitational waves interferometers, Opt. Lett. **36**, 1407 (2011).
[20] E. O. Inc, Anti-reflection(ar) coatings, https://www.edmundoptics.com/knowledge-center/application-notes/lasers/anti-reflection-coatings/.
[21] C. Eaglesfield, Mode-conversion loss in a sequential confocal lens system, in *Proceedings of the Institution of Electrical Engineers* (IET, London, 1964), Vol. 111, pp. 610–615, 10.1049/piee.1964.0109.
[22] F. K. Schwering, On the theory of randomly misaligned beam waveguides, IEEE Trans. Microwave Theory Tech. **15**, 206 (1967).
[23] W. H. Steier, The statistical effects of random variations in the components of a beam waveguide, Bell Syst. Tech. J. **45**, 451 (1966).
[24] J. Christian, G. Goubau, and J. Mink, 5.6-self-aligning optical beam waveguides+ c6553, IEEE J. Quantum Electron. **3**, 498 (1967).
[25] W. Herrmannsfeldt, M. Lee, J. Spranza, and K. Trigger, Precision alignment using a system of large rectangular fresnel lenses, Appl. Opt. **7**, 995 (1968).
[26] P. Fritschel, N. Mavalvala, D. Shoemaker, D. Sigg, M. Zucker, and G. González, Alignment of an interferometric gravitational wave detector, Appl. Opt. **37**, 6734 (1998).

[27] G. Herziger and H. Weber, Equivalent optical resonators, Appl. Opt. **23**, 1450_1 (1984).
[28] R. Schnabel, M. Britzger, F. Brückner, O. Burmeister, K. Danzmann, J. Duck, T. Eberle, D. Friedrich, H. Luck, M. Mehmet *et al.*, Building blocks for future detectors: Silicon test masses and 1550 nm laser light, J. Phys. Conf. Ser. **228**, 012029 (2010).
[29] M. H. Liyuan Zhang and G. Billingsley, Itm09hr ar absorption, LIGO Document No. 1300674, 2013.
[30] K. Predehl, G. Grosche, S. Raupach, S. Droste, O. Terra, J. Alnis, T. Legero, T. Hänsch, T. Udem, R. Holzwarth *et al.*, A 920-kilometer optical fiber link for frequency metrology at the 19th decimal place, Science **336**, 441 (2012).
[31] M. Schioppo, J. Kronjaeger, A. Silva, R. Ilieva, J. Paterson, C. Baynham, W. Bowden, I. Hill, R. Hobson, A. Vianello *et al.*, Comparing ultrastable lasers at 7×10^{-17} fractional frequency instability through a 2220 km optical fibre network, Nat. Commun. **13**, 212 (2022).
[32] S. M. Foreman, K. W. Holman, D. D. Hudson, D. J. Jones, and J. Ye, Remote transfer of ultrastable frequency references via fiber networks, Rev. Sci. Instrum. **78**, 021101 (2007).
[33] M. Kakui, M. Matsui, T. Saitoh, and Y. Chigusa, Ultra-low-loss (0.1484 db/km) pure silica core fibre and extension of transmission distance, Electron. Lett. **38**, 1168 (2002).
[34] H. Sakr, T. D. Bradley, G. T. Jasion, E. N. Fokoua, S. R. Sandoghchi, I. A. Davidson, A. Taranta, G. Guerra, W. Shere, Y. Chen *et al.*, Hollow core NANFs with five nested tubes and record low loss at 850, 1060, 1300 and 1625 nm, in *Optical Fiber Communication Conference* (Optica Publishing Group, Washington, 2021), pp. F3A–4, 10.1364/OFC.2021.F3A.4.
[35] R. V. Kochanov, I. Gordon, L. Rothman, P. Wcisło, C. Hill, and J. Wilzewski, Hitran application programming interface (hapi): A comprehensive approach to working with spectroscopic data, J. Quant. Spectrosc. Radiat. Transfer **177**, 15 (2016).
[36] M. Greenspan, Transmission of sound waves in gases at very low pressures, in *Properties of Gases, Liquids, and Solutions*, Physical Acoustics Vol. 2, edited by W. P. Mason (Academic Press, New York, 1965), pp. 1–45.
[37] K. L. Dooley, L. Barsotti, R. X. Adhikari, M. Evans, T. T. Fricke, P. Fritschel, V. Frolov, K. Kawabe, and N. Smith-Lefebvre, Angular control of optical cavities in a radiation-pressure-dominated regime: The enhanced LIGO case, J. Opt. Soc. Am. A **30**, 2618 (2013).
[38] A. S. Holevo and R. F. Werner, Evaluating capacities of bosonic Gaussian channels, Phys. Rev. A **63**, 032312 (2001).
[39] K. Noh, V. V. Albert, and L. Jiang, Improved quantum capacity bounds of Gaussian loss channels and achievable rates with Gottesman-Kitaev-Preskill codes, IEEE Trans. Inf. Theory **65**, 2563 (2019).
[40] C.-H. Wang, F. Li, and L. Jiang, Quantum capacities of transducers, Nat. Commun. **13**, 6698 (2022).
[41] Y.-A. Chen *et al.*, An integrated space-to-ground quantum communication network over 4,600 kilometres, Nature (London) **589**, 214 (2021).
[42] C.-Y. Lu, Y. Cao, C.-Z. Peng, and J.-W. Pan, Micius quantum experiments in space, Rev. Mod. Phys. **94**, 035001 (2022).
[43] K. Azuma, S. E. Economou, D. Elkouss, P. Hilaire, L. Jiang, H.-K. Lo, and I. Tzitrin, Quantum repeaters: From quantum networks to the quantum internet, Rev. Mod. Phys. **95**, 045006 (2023).
[44] H.-K. Lo, M. Curty, and B. Qi, Measurement-device-independent quantum key distribution, Phys. Rev. Lett. **108**, 130503 (2012).
[45] Y. Liu, T.-Y. Chen, L.-J. Wang, H. Liang, G.-L. Shentu, J. Wang, K. Cui, H.-L. Yin, N.-L. Liu, L. Li *et al.*, Experimental measurement-device-independent quantum key distribution, Phys. Rev. Lett. **111**, 130502 (2013).
[46] M. Lucamarini, Z. L. Yuan, J. F. Dynes, and A. J. Shields, Overcoming the rate-distance limit of quantum key distribution without quantum repeaters, Nature (London) **557**, 400 (2018).
[47] S. Wang, Z.-Q. Yin, D.-Y. He, W. Chen, R.-Q. Wang, P. Ye, Y. Zhou, G.-J. Fan-Yuan, F.-X. Wang, W. Chen *et al.*, Twin-field quantum key distribution over 830-km fibre, Nat. Photonics **16**, 154 (2022).
[48] A. K. Ekert, Quantum cryptography based on Bell's theorem, Phys. Rev. Lett. **67**, 661 (1991).
[49] P. Sekatski, J.-D. Bancal, X. Valcarce, E. Y.-Z. Tan, R. Renner, and N. Sangouard, Device-independent quantum key distribution from generalized chsh inequalities, Quantum **5**, 444 (2021).
[50] F. Xu, Y.-Z. Zhang, Q. Zhang, and J.-W. Pan, Device-independent quantum key distribution with random post-selection, Phys. Rev. Lett. **128**, 110506 (2022).
[51] W.-Z. Liu, Y.-Z. Zhang, Y.-Z. Zhen, M.-H. Li, Y. Liu, J. Fan, F. Xu, Q. Zhang, and J.-W. Pan, Toward a photonic demonstration of device-independent quantum key distribution, Phys. Rev. Lett. **129**, 050502 (2022).
[52] P. Komar, E. M. Kessler, M. Bishof, L. Jiang, A. S. Sorensen, J. Ye, and M. D. Lukin, A quantum network of clocks, Nat. Phys. **10**, 582 (2014).
[53] J. Liu, C. T. Hann, and L. Jiang, Data centers with quantum random access memory and quantum networks, Phys. Rev. A **108**, 032610 (2023).
[54] S. Barz, E. Kashefi, A. Broadbent, J. F. Fitzsimons, A. Zeilinger, and P. Walther, Demonstration of blind quantum computing, Science **335**, 303 (2012).
[55] J. F. Fitzsimons, Private quantum computation: An introduction to blind quantum computing and related protocols, npj Quantum Inf. **3**, 23 (2017).